

## Shock-Induced Anisotropy in Ferromagnetic Material. II. Polycrystalline Behavior and Experimental Results for YIG<sup>†</sup>

D. E. Grady\* and G. E. Duvall

*Washington State University, Pullman, Washington 99163*

and

E. B. Royce

*Lawrence Radiation Laboratory, University of California, Livermore, California 94550*

(Received 21 June 1971; in final form 6 December 1971)

The theory of shock-induced demagnetization produced by strain-induced magnetic anisotropy is considered in cubic polycrystalline ferromagnetic material. Analysis of the averaging procedure required to predict the polycrystalline behavior reveals the importance of magnetic grain interaction. Magnetization curves for extreme assumptions of interacting grains and independent grains are determined. Experimental shock demagnetization data are obtained for polycrystalline yttrium iron garnet in the region of large elastic strain (approximately  $\frac{1}{3}$  and  $\frac{2}{3}$  of the Hugoniot elastic limit). Results support the independent grain assumption.

### I. INTRODUCTION

Previous experimental work on magnetic shock-induced anisotropy has been, without exception, on polycrystalline ferromagnetic or ferrimagnetic material.<sup>1-5</sup> In polycrystalline material, the single-crystal shock-induced anisotropy discussed in the preceding paper<sup>6</sup> oc-

curs in individual crystallites. Primary concerns of the present work are the prediction of average polycrystalline magnetic behavior and the magnetic interaction between grains which must be known or assumed before the average behavior can be predicted unambiguously. Previous theoretical work on shock-induced anisotropy

in polycrystalline materials has assumed, for the sake of expedience, uniform magnetization within the material.<sup>3,7</sup> This assumes a substantial magnetic interaction between grains and is not necessarily the correct assumption. In the present work extreme assumptions concerning the magnetic grain interaction are formulated. They are referred to as the interacting grain and independent grain assumptions, respectively. Polycrystalline magnetic behavior is determined for each assumption.

Actual magnetic behavior will be bounded by the two extreme predictions. Experimental objectives of the present work are to determine which magnetic behavior predicted from the extreme assumptions concerning magnetic grain interaction more closely represents actual behavior. Experimental shock demagnetization curves for polycrystalline yttrium iron garnet were obtained with the gas gun facilities at Washington State University. Data obtained in the region of large elastic strain (approximately  $\frac{1}{3}$  and  $\frac{2}{3}$  of the Hugoniot elastic limit) support the independent grain assumption. From these results, conclusions concerning relative contributions of the various energy terms affecting the magnetic behavior are obtained.

In Sec. II, the general polycrystalline averaging procedure is briefly summarized. Shock demagnetization curves are then obtained for the interacting grain and independent grain assumptions. The physics implied by each assumption is discussed. The experimental method and material characterization are reported in Sec. III. In Sec. IV, the experimental results are presented. In Sec. V, results are discussed in terms of the magnetic energies contributing to the shock-induced anisotropy effect.

## II. THEORY

The prediction of a polycrystalline material property from its equivalent single-crystal property is a problem confronted in many areas of physics. The approach, quite similar in every case, requires an averaging of the single-crystal property for an arbitrarily oriented crystallite over all crystal orientations.<sup>8</sup> A complicating factor is that an arbitrary crystallite interacts not only with the external forces but also with other grains in the polycrystalline material. This grain interaction can be mechanical (through stresses), electrical, or magnetic. In most cases, the interaction is not understood.

Examples of such material properties are elastic constants, dielectric constants, magnetostriction constants, and conductivities. In each case, basic assumptions concerning the grain interaction must be formulated before progress can be made. For instance, in the case of elastic constants two extreme assumptions have been used. One assumption is that uniform strain exists throughout the polycrystal.<sup>9</sup> The other is that uniform stress prevails.<sup>10</sup> Experiment favors neither, usually being closer to an arithmetic average of the results of the two assumptions.<sup>11</sup> Similar assumptions are made in obtaining polycrystalline magnetostriction constants.<sup>12-15</sup>

In the present problem, the state of strain behind a

plane shock wave in a theoretically dense cubic polycrystal is assumed uniform.<sup>16</sup> The speculation of present interest concerns the magnetic grain interaction. This is an interaction of current interest about which little is known.<sup>17-18</sup> In analogy with the method used to obtain polycrystalline elastic constants, this development will define extreme assumptions concerning the magnetic grain interaction and then consider each individually.

One extreme is that material crystallites interact with sufficient strength to cause a cooperative collinear alignment of the magnetization vectors throughout the specimen. The other extreme is that magnetic grain interaction is negligible and that each grain individually seeks equilibrium determined only by the requirements of the induced anisotropy field and external magnetic field. These assumptions will be called the interacting grain assumption and the independent grain assumption, respectively.

### A. Interacting Grain Assumption

The interacting grain assumption used by Shaner and Royce<sup>3,4</sup> during early work on shock-induced anisotropy leads to a mathematically tractable averaging process. Domain structure in a polycrystalline ferromagnet is usually on an intragrain scale. This is due to high crystal anisotropy energy and large-angle grain boundaries which make continuous domains across grain boundaries energetically unfavorable. There are cases, however, such as in material subject to cold working, in which a degree of crystal orientation allows an extragrain domain structure.<sup>19</sup> In the present effect, the easy direction of magnetization is determined not only by the crystallographic axis, but also by the axis of uniaxial strain.<sup>20</sup> Thus, the effect of the shock wave is to create a condition of magnetic texture defined by the direction of uniaxial strain behind the shock wave. It might be reasonable to expect an extragrain domain structure to nucleate after passage of the shock wave.

Continuing this argument, consider a spherical grain within a domain of uniform magnetization. Magnetization in this grain could deviate from the direction of uniform magnetization only by creating surface poles on the grain boundary. The energy associated with this is

$$E = \frac{4}{3}\pi M_s^2 \cos\gamma,$$

where  $M_s$  is the saturation magnetization and  $\gamma$  is the angle defining the deviation of the grain's magnetization from the direction of uniform magnetization. In YIG, at typical shock stresses, this energy is of the same order as the strain-induced anisotropy energy. Hence, there would be strong torques attempting to maintain uniform magnetization throughout a domain.

The interacting grain assumption is  $M \cdot H$  is uniform throughout the field. This simply states that the projection  $M_s \cos\theta$  along the direction of the applied field is constant for arbitrary crystal orientation. Prediction of the magnetization curve requires construction of an appropriate energy expression. This will consist of the interaction energy

$$E_H = -M \cdot H_e \quad (1)$$

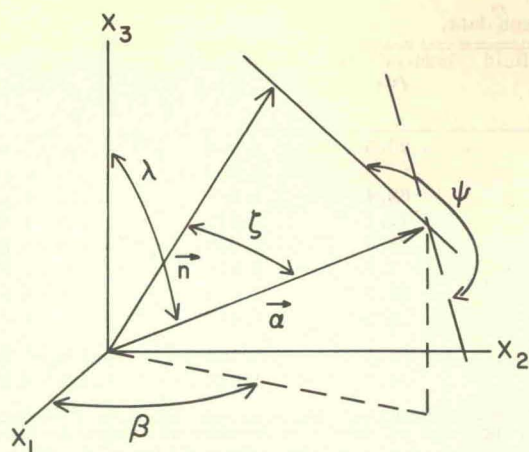


FIG. 1. Independent angular coordinates for representing strain-induced anisotropy energy.  $\alpha$  determines magnetization axis.  $n$  determines strain axis.  $\psi$  represents rotation of plane defined by  $\alpha$  and  $n$  about axis determined by  $\alpha$ .

and the induced anisotropy energy

$$E_{me} = b_1 e (\alpha_1^2 n_1^2 + \alpha_2^2 n_2^2 + \alpha_3^2 n_3^2) + 2b_2 e (\alpha_1 \alpha_2 n_1 n_2 + \alpha_2 \alpha_3 n_2 n_3 + \alpha_3 \alpha_1 n_3 n_1). \quad (2)$$

In this expression the uniaxial strain tensor  $e_{ij} = en_i n_j$  is used. The exchange and demagnetizing energies are considered implicitly in the assumption of uniform magnetization. If this assumption is correct their contribution is considerable. The crystal anisotropy is ignored. It is small in the region of strains considered.

To proceed with the averaging process, the six variables  $\alpha_1$ ,  $\alpha_2$ ,  $\alpha_3$ ,  $n_1$ ,  $n_2$ , and  $n_3$  ( $\alpha$  and  $n$  are unit vectors) are expressed in terms of four independent angular variables as shown in Fig. 1.<sup>21</sup> Direction cosines are related to the angular variables by

$$\begin{aligned} \alpha_1 &= \sin \lambda \cos \beta, & \alpha_2 &= \sin \lambda \sin \beta, & \alpha_3 &= \cos \lambda, \\ n_1 &= \cos \xi \sin \lambda \cos \beta + \sin \xi (\cos \lambda \cos \beta \cos \psi + \sin \beta \sin \psi), \\ n_2 &= \cos \xi \sin \lambda \sin \beta + \sin \xi (\cos \lambda \sin \beta \cos \psi - \cos \beta \sin \psi), \end{aligned}$$

and

$$n_3 = \cos \xi \cos \lambda - \sin \xi \sin \lambda \cos \psi.$$

Assuming the polycrystal is isotropic,

$$\frac{1}{8}\pi^{-2} \sin \lambda \, d\lambda \, d\beta \, d\psi$$

is the probability that the magnetization lies in the range  $\lambda$  to  $\lambda + d\lambda$  and  $\beta$  to  $\beta + d\beta$ , while the strain axis lies in a range  $\psi$  to  $\psi + d\psi$ . The average values of the terms appearing in the energy expression are obtained from

$$\bar{f}(\xi) = \frac{1}{8}\pi^{-2} \int_0^\pi \int_0^{2\pi} \int_0^{2\pi} f(\xi, \lambda, \beta, \psi) \sin \lambda \, d\lambda \, d\beta \, d\psi. \quad (3)$$

The resulting average induced anisotropy energy is

$$E_{me} = B e \cos^2 \xi,$$

where  $B = \frac{2}{5}b_1 + \frac{3}{5}b_2$ , or in terms of the usual magnetostriction coefficients

$$B = -\frac{3}{5}[(C_{11} - C_{12})\lambda_{100} + 3C_{44}\lambda_{111}].$$

It is instructive to recall that these formulas have been derived under the assumption that the strains are identical in all grains. This assumption leads to a polycrystalline magnetostriction coefficient

$$\lambda = \frac{(C_{11} - C_{12})\lambda_{100} + 3C_{44}\lambda_{111}}{3C_{44} + C_{11} - C_{12}},$$

the fractional striction of a material along the direction in which it is magnetized. This formula may be compared with the usual polycrystalline magnetostriction formula

$$\lambda = \frac{2}{5}\lambda_{100} + \frac{3}{5}\lambda_{111},$$

derived under the assumption that each grain behaves independently mechanically. Obviously, for isotropy ( $C_{11} - C_{12} = 2C_{44}$ ), the two formulas are identical.

The angle  $\theta$  between the direction of the applied field and the direction of the magnetization is the complement of  $\xi$ . The total thermodynamic energy expression becomes

$$E = B e \sin^2 \theta - H_e M_s \cos \theta. \quad (4)$$

The magnetization curve obtained from Eq. (4) for positive magnetoelastic constants is

$$\begin{aligned} M/M_s &= 1, & H_e &> -2Be/M_s \\ &= -(M_s/2Be)H_e, & H_e &< -2Be/M_s. \end{aligned} \quad (5)$$

This is intermediate between the extremes obtained for the  $\langle 100 \rangle$  problem and the  $\langle 111 \rangle$  problem for the equivalent single-crystal behavior derived in the preceding paper.<sup>6</sup>

#### B. Independent Grain Assumption

It is quite possible that the uniform magnetization field demanded by the previous assumption does not occur. The isolated single-particle critical size within which a single domain exists for YIG is less than  $1 \mu$ . This critical size will increase for a bounded crystallite due

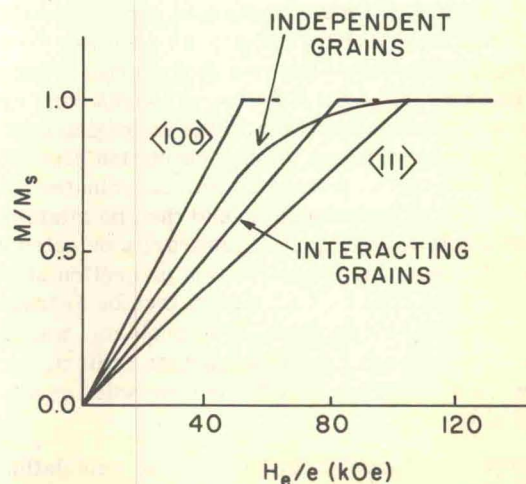


FIG. 2. Magnetization curves in polycrystalline YIG predicted from the independent and interacting grain theories. Shown for comparison are the single-crystal magnetization curves from the  $\langle 100 \rangle$  and  $\langle 111 \rangle$  problems.

TABLE I. Shock demagnetization data.

Shot No.	Projectile velocity (mm/ $\mu$ sec)	Projectile material	Mean strain in YIG	Magnetic field (Oe)	Induced <sup>a</sup> emf (V)	Specimen width (cm)	$\delta M/M_s$ <sup>b</sup>
70-016	0.598			359	20.5	1.060	0.332 $\pm$ 0.066
70-030 <sup>c</sup>	0.602			245	...	1.063	0.602 $\pm$ 0.100
70-039	0.600	Plexiglass		258	62.4	1.067	0.515 $\pm$ 0.033
70-053	0.601	Rohm		588	11.2	1.075	0.089 $\pm$ 0.034
70-057	0.596	and	-0.0083	494	21.6	1.085	0.173 $\pm$ 0.037
70-059	0.598	Haas		680	4.6	1.081	0.039 $\pm$ 0.015
71-002	0.597	type-G		421	30.3	1.023	0.260 $\pm$ 0.055
71-013	0.598			787	2.5	1.081	0.018 $\pm$ 0.010
71-015	0.551	Aluminum		660	48.5	1.068	0.400 $\pm$ 0.030
71-016	0.555	oxide	-0.0162	935	20.5	1.032	0.173 $\pm$ 0.038
		WESGO-995					

<sup>a</sup>This emf was developed across 10-turn pickup coils with the exception of shot No. 70-016 which used a 5-turn pickup coil.

<sup>b</sup>Calculated with an  $M_s$  of 128 G.

<sup>c</sup>On this shot, the solenoid was prematurely shorted. These values were obtained by estimating the field due to residual current and knowledge of the circuit inductances and resistances.

to a substantial decrease in surface magnet poles at the grain boundary, but not by more than an order of magnitude.<sup>17</sup> The grain size of the material used in the present work ranges from 5 to 25  $\mu$ . This suggests that perhaps an intragrain domain structure will nucleate in order to reduce magnetic poles which would otherwise collect heavily along grain boundaries.<sup>17,22</sup> This latter case holds if the energy associated with domain walls is small compared to other magnetic energies. With an intragrain domain structure there is not a uniform magnetization field as was demanded by the interacting grain assumption. In this case, it is more likely that the magnetization in each grain independently seeks a value depending only on the orientation of its crystallographic axis with the external fields.

A simple consideration shows that the independent grain assumption leads to a lower average magnetoelastic energy than the interacting grain theory. The energy from the interacting grain theory contained a part required to bring individual grains into their independent equilibrium positions and also a part required to bring these grains into collinear alignment. The latter contribution would not be present in the independent grain assumption.

The independent grain assumption is *each crystallite seeks equilibrium subject only to the requirements of the induced anisotropy field and the external magnetic field, independent of the behavior of neighboring crystallites*. A rigorous approach to the averaging procedure would be to express the magnetization direction cosines in Eq. (2) in terms of polar coordinates  $\lambda$  and  $\beta$ . The total energy expression should then be minimized with respect to  $\lambda$  and  $\beta$  for an arbitrarily oriented crystallite. The resulting magnetization projection along the direction of the applied field should then be averaged over all crystal orientations. This problem, which has been encountered previously in another context, cannot be solved explicitly for  $\lambda$  and  $\beta$  and the solution has not been completed.<sup>14</sup>

An alternative approach, in the spirit of calculations made by Lee,<sup>23</sup> is to write the average normalized magnetization

$$M/M_s = (\cos\theta)_{av} = \int F(\Omega) \cos\theta d\Omega / (\int F(\Omega) d\Omega)^{-1} \quad (6)$$

in terms of an unknown distribution function.  $F(\Omega)$  is the

equilibrium distribution of magnetization directions over all crystal orientations for a given applied field  $H_e$  and state of strain  $e$ . The following distribution function is assumed:

$$F(\Omega) = 1, \quad \theta_1 < \theta < \theta_2 \quad (7)$$

$$= 0, \quad \text{otherwise.}$$

The angles  $\theta_1$  and  $\theta_2$  are the extremes defined by the  $\langle 100 \rangle$  problem and the  $\langle 111 \rangle$  problem in the preceding paper. They are

$$\cos\theta_1 = (M_s/2b_1e)H_e \quad (8)$$

and

$$\cos\theta_2 = (M_s/2b_2e)H_e. \quad (9)$$

A similar distribution function has been used by Bozorth<sup>24</sup> in an attempt to explain low-remanence values in certain alloys and by Lee<sup>23</sup> to explain magnetostriction curves over the whole range of magnetization to saturation. In the work of Lee,<sup>23</sup> results using the uniform distribution function and a distribution function predicted theoretically by Brown<sup>25</sup> were compared. Experimental data strongly supported the uniform distribution function.

It must be realized that this approach will yield an approximate solution to a problem which has not, as yet, been solved exactly. The prediction is subject to the limitations of this assumption. Equation (6) becomes

$$(\cos\theta)_{av} = \int_{\theta_1}^{\theta_2} \cos\theta \sin\theta d\theta / (\int_{\theta_1}^{\theta_2} \sin\theta d\theta)^{-1}$$

$$= \int_{x_2}^{x_1} x dx / (\int_{x_2}^{x_1} dx)^{-1}, \quad (10)$$

where  $x = \cos\theta$ . A problem occurs when  $\cos\theta_1$  is unity, at which point the first grains reach saturation. To freeze the upper limit of integration artificially constrains the distribution function. This problem can be circumvented by allowing the upper limit to continue but demanding that the respective contribution to  $(\cos\theta)_{av}$  be unity. This gives

$$(\cos\theta)_{av} = (\int_{x_2}^1 x dx + \int_1^{x_1} dx) / (\int_{x_2}^{x_1} dx)^{-1}, \quad x_2 \leq 1 \leq x_1$$

$$= \int_{x_2}^{x_1} x dx / (\int_{x_2}^{x_1} dx)^{-1}, \quad x_1 < 1. \quad (11)$$

Performing the required integration, the predicted

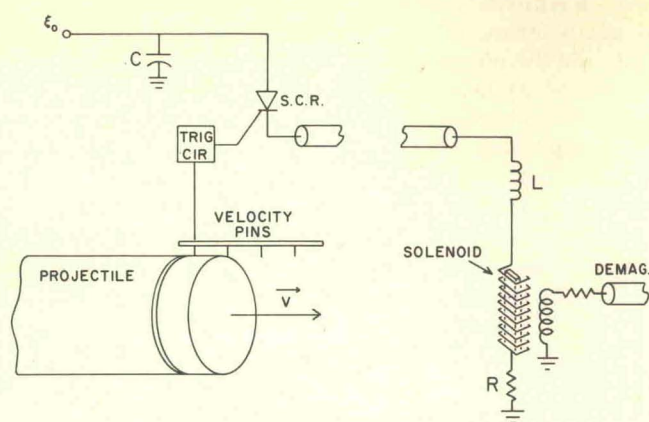


FIG. 3. Schematic representation of experimental method. Current supply is triggered by projectile contact with velocity pin. Planar impact occurs between projectile and solenoid when current (hence magnetic field) in solenoid is maximum.

magnetization curve for the independent grain assumption is

$$\begin{aligned} M/M_s &= 1, & x_2 > 1 \\ &= \frac{1}{2}(x_1 + x_2) - \frac{1}{2}(x_1 - 1)^2/(x_1 - x_2), & x_2 \leq 1 \leq x_1, \quad (12) \\ &= \frac{1}{2}(x_1 + x_2), & x_1 < 1, \end{aligned}$$

where

$$x_1 = -(M_s/2b_1e)H_e \text{ and } x_2 = -(M_s/2b_2e)H_e. \quad (13)$$

The predicted magnetization curve for the independent grain theory is qualitatively pleasing for two reasons. First, the magnetization curve tends initially toward saturation more rapidly than is predicted by the interacting grain theory. This behavior is expected because of the excessive energy attributed to the magnetoelastic energy in the interacting grain theory. Secondly, the curve approaches saturation gradually as would be the case if all grains were not forced to saturation simultaneously. In the case of magnetoelastic isotropy ( $b_1 = b_2$ ), the magnetization curve for the independent grain theory is coincident with that of the interacting grain theory. Predicted magnetization curves in YIG for the two theories [Eqs. (5) and (12)] along with those for the  $\langle 100 \rangle$  and  $\langle 111 \rangle$  problems from the preceding paper are shown in Fig. 2.

### III. EXPERIMENTAL METHOD

The experimental method used to obtain shock demagnetization curves and test the theories developed in Sec. II will be briefly described here.<sup>26</sup> The theory requires an infinite slab of ferromagnetic material subject to a state of uniaxial strain normal to the plane of the slab and an applied magnetic field in the plane of the slab. This was approximated by a rectangular specimen of polycrystalline yttrium iron garnet. The uniaxial strain was obtained by planar impact of a projectile from a 4-in. gas gun.<sup>27</sup> The magnetic field was applied by pulsing a current through a rectangular solenoid enveloping the specimen.

A schematic representation of the experimental procedure is illustrated in Fig. 3. The experimental sequence is as follows: The projectile, travelling at a velocity  $V$  triggers the current supply. The subsequent current produces a magnetic field which reaches a maximum and is quasistatic at the time the projectile impacts the target. The current profile is determined by the LCR characteristics of the circuit. The impact produces a strain wave which propagates through the solenoid and into the YIG sample. This sample, initially in magnetic saturation, is demagnetized by the strain wave. The demagnetization develops an emf across the pickup coil, shown schematically in Fig. 3, which is recorded on the monitoring oscilloscopes. Demagnetization of the ferromagnetic material behind the shock wave is determined from these records.

Measurement of the applied magnetic field is made by monitoring the current through a precision noninductive resistor in series with the solenoid. Fields from 200 to 1000 Oe were required in this work. The state of uniaxial strain in the YIG is determined from the measured projectile velocity and the Hugoniot equations of state for the projectile material, intermediate material,<sup>28,29</sup> and magnetic material<sup>30</sup> (Lucite, Lucite, and YIG, respectively, for the first series in Table I). Strains corresponding to about  $\frac{1}{3}$  and  $\frac{2}{3}$  the Hugoniot elastic limit were produced in the YIG.

The demagnetization records are obtained from the emf developed across a 10-turn pickup coil closely wound around the center of the rectangular YIG specimen. The induced emf is related to the change in magnetization by considering the jump in magnetic flux across a steady-state shock wave. Analysis is similar to that used to obtain mechanical shock-wave jump conditions.<sup>31</sup> The result is

$$\frac{d\Phi}{dt} = 4\pi bD\Delta M - buH_e, \quad (14)$$

where  $\Phi$  is the magnetic flux,  $b$  is the width of the magnetic specimen and pickup coil,  $D$  is the shock velocity, and  $u$  is the particle velocity behind the shock wave. In this work, the  $buH_e$  contribution was small compared to the first term.  $\Delta M = M - M_s$ , the change in magnetization per unit initial volume, determines the state of magnetization in the material behind the shock front. In other words, the demagnetization in the material, subject to a given applied field  $H_e$  and induced uniaxial strain  $e$ , is obtained from the measured emf with Eq. (14) and Faraday's law. A representative demagnetization record is shown in Fig. 4.

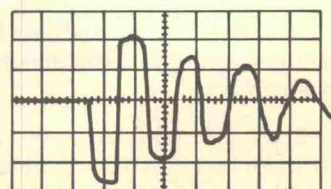


FIG. 4. Oscilloscope record of shock-induced demagnetization in YIG. Periodicity corresponds to reverberation of stress wave in YIG platelet. Time scale is  $0.2 \mu \text{sec/div}$ .

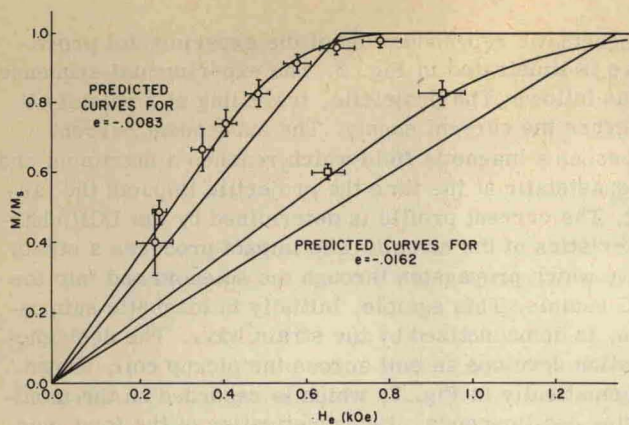


FIG. 5. Experimental data with theoretical magnetization curves for two strain-induced anisotropy fields. Circles correspond to strain of  $-0.0083$ . Squares correspond to strain of  $-0.0162$ . Smooth curves correspond to independent grain theory. Curves with slope discontinuity correspond to interacting grain theory.

The material selected for this study was hot-pressed polycrystalline yttrium iron garnet.<sup>32</sup> It was chosen because the magnetoelastic properties are of convenient magnitude for shock-wave investigation. Also this was the material used by Shaner and Royce in earlier investigation of shock-induced demagnetization at high stresses.<sup>3</sup> Important points noted during material characterization are the following: Photomicrographs showed the average grain size to be approximately  $15 \mu$  varying from 5 to  $25 \mu$ . The grain distribution was visually homogeneous and isotropic throughout the sample; i. e., there was no evidence of mechanical texture created by the hot-pressing process. The porosity was  $3.3 \pm 0.5\%$ . Pores were highly spherical and observed to occur both intragranularly and at grain boundaries. The specimens were lapped flat and parallel to dimensions of  $0.1 \times 1.0 \times 5.0$  cm. Values used for the magnetoelastic constants were  $b_1 = 3.5 \times 10^6$  erg/cm<sup>3</sup> and  $b_2 = 6.9 \times 10^6$  erg/cm<sup>3</sup>.<sup>30</sup> The value used for the theoretically dense saturation magnetization was 133.7 G.<sup>33</sup> The value for the present, slightly porous materials, was 128 G.

#### IV. EXPERIMENTAL RESULTS

Experimental data are presented in Table I and plotted in Figs. 5 and 6. The strain in the first series corresponds to a longitudinal stress of 22 kbar, the second series to a longitudinal stress of 43 kbar. The Hugoniot elastic limit in YIG is 62 kbar (attributed to Graham).<sup>34</sup> Experimental magnetization curves are shown in Fig. 5 along with theoretical curves for the interacting grain and independent grain assumptions. In Fig. 6 the data are plotted as a function of the normalized field  $H_e/e$  against which the predicted magnetization curves for any state of strain are self-similar.

It is observed in Figs. 5 and 6 that the two alternative theories differ at most by about 15% in absolute value of magnetization. The measured quantity, however, is the reduction in magnetization or demagnetization. The alternative theories are quite sensitive to this quantity in the upper region of the magnetization curve.

As was mentioned previously, the state of strain in the YIG was determined from equation-of-state knowledge of YIG and the intermediate materials. The accuracy of this method might be questioned since Lucite, a material with known viscoelastic response,<sup>28</sup> is used. To alleviate this problem, the propagation distance through Lucite from impact to the YIG interface was kept to a minimum. To test the analysis quartz gauges were substituted at the YIG interface in several experiments. This allowed comparison of calculated strain with measured strain in the quartz. In no case was the difference greater than 4%. The error in the applied field  $H_e$  was  $\pm 2\%$ . Strictly, this was the error in measuring the solenoid current during shock transit. This method was not suspect and no attempt was made to measure the field directly. The horizontal error bars in Figs. 5 and 6 are  $\pm 6\%$ .

The demagnetization profile in Fig. 3 is observed to exhibit some structure. This structure is typical of all the experimental records. The behavior is due to the finite rise in the strain pulse ( $\sim 50$  nsec) and lateral relief waves produced by the finite width of the YIG slabs. An analytic estimate of the structure was made and found consistent with the records. This analysis, however, was not relied on to reduce the error in the experiment. In each profile quite evident extremes occurred to bound the actual demagnetization. These extremes were accepted as error and define the vertical error bars in Figs. 5 and 6 and are the errors quoted in the right-hand column of Table I. This was by far the dominant error. Values for the saturation magnetization in YIG vary from about 128 to 140 G in the literature. The data are not sensitive to this difference.

#### V. DISCUSSION AND CONCLUSIONS

The data presented in Figs. 5 and 6 support the shock-induced anisotropy mechanism as a contribution to shock demagnetization. It is further concluded that the independent grain assumption provides a better description of the magnetic behavior of polycrystalline ferromagnetic material in the shocked state. Also established

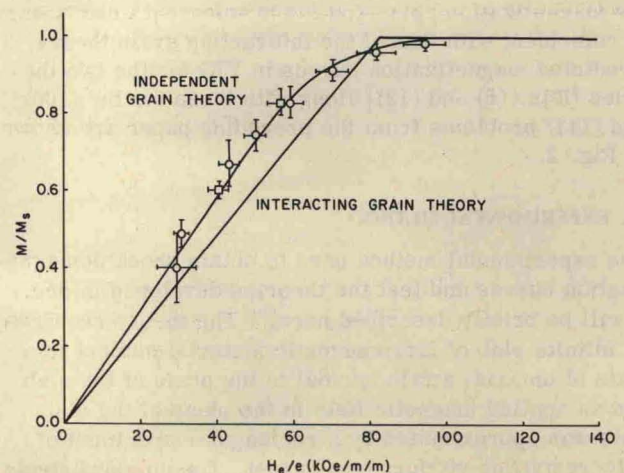


FIG. 6. Data plotted to exhibit theoretically predicted self-similarity of magnetization curves against the parameter  $H_e/e$ .

is the validity of the parameter  $H_e/e$  in characterizing the magnetization curve. This is seen in Fig. 6 where the experimental magnetization curves, plotted as a function of this parameter, are self-similar.

In retrospect, independent grain behavior appears more reasonable than interacting grain behavior. In the previous article,<sup>6</sup> the equilibrium exchange and demagnetizing energy was predicted to increase as the fourth root of the strain. It was further predicted to be small compared to the induced anisotropy energy. It follows that the energy of domain walls is small and an intra-grain domain structure would occur. Considering this, one would expect independent grain behavior. Conversely, experimental agreement with the independent grain theory adds support to the validity of the calculation which predicts the negligible contribution of the equilibrium exchange and demagnetizing energy at the magnitude of strain occurring in this work.

The prediction of magnetic behavior behind the shock front is much simpler than the equivalent prediction in unstrained material. First, the equilibrium exchange and demagnetizing energy can be ignored in favor of the much simpler induced anisotropy energy. This is not the case in unstrained material. Second, in polycrystalline material the magnetic grain interaction effects are not substantial and magnetic properties can be obtained by averaging the behavior of a single independent grain.

It was stated in Sec. III that the magnetic material used in this work had a slight porosity. This is typical of most magnetic ceramics. Wayne *et al.*<sup>35</sup> have reported that the macroscopic magnetization of porous magnetic material subject to hydrostatic pressure is affected due to nonhydrostatic strains occurring in the vicinity of pores. It seems evident that this effect should occur in the uniaxial strain case also. Calculations predict that the effect of porosity on the magnetization curves obtained in the present work will be small for large applied fields but become substantial as the applied field approaches zero.<sup>36</sup> The region of the magnetization curve experimentally observed was chosen to circumvent the porosity problem.

Contribution to the shock-induced anisotropy effect due to finite strain was calculated.<sup>36</sup> This was demanded by the high strains obtained in the present work. Calculations show that the contribution is not substantial. The experimental data verify this conclusion. It follows that, at least for the present material and experimental accuracy, the conventional magnetoelastic theory of Becker and Doring provides an adequate description of shock-induced anisotropy in the region of large elastic strain.

The present work seems to be consistent with previous data on YIG obtained by Shaner and Royce.<sup>3</sup> Their 90-kbar data, which are twice the highest stress obtained in this work and about 30 kbar above the Hugoniot elastic limit, fall slightly above the predicted magnetization curve for the independent grain theory. Their 200- and 440-kbar data are higher yet. Their data are compared with the present work by assuming a simple elastic-plastic model for the behavior above the Hugoniot elastic limit. This discrepancy has been discussed recently by Royce<sup>4</sup> and is attributed to the effect of porosity and to

the change in saturation magnetization for the higher-pressure data.

## VI. SUMMARY

The conclusions reached and results obtained during the course of this work are as follows:

- (i) Consideration of the averaging process required to predict the shock-induced anisotropy effect in polycrystalline material reveals the importance of magnetic grain interaction. Extreme assumptions of interacting grains and independent grains are defined to describe this interaction. Magnetization curves are obtained for both assumptions.
- (ii) Data on polycrystalline yttrium iron garnet were obtained in the region of large elastic strain. The results support the independent grain theory as more representative of actual magnetic behavior. Earlier theoretical work assumed interacting grain behavior.
- (iii) The experimental results are in agreement with the domain-theory analysis of the preceding paper which predicts the negligible contribution from exchange and demagnetizing effects.
- (iv) Conventional magnetoelastic theory provides a sufficient characterization of the shock-induced anisotropy effect within present experimental accuracy for strains up to at least  $\frac{2}{3}$  the Hugoniot elastic limit.

\*Present address: Stanford Research Institute, Menlo Park, Calif.

<sup>†</sup>Based on a thesis submitted to the Department of Physics, Washington State University, Pullman, Wash., in partial fulfillment of the Doctor of Philosophy degree, 1971. Work supported by the Air Force Office of Scientific Research, Grant No. AFOSR 69-1758.

<sup>1</sup>E. B. Royce, *J. Appl. Phys.* **37**, 4066 (1966).

<sup>2</sup>E. B. Royce, in *Behavior of Dense Media under High Dynamic Pressures* (Gordon and Breach, New York, 1968), p. 419.

<sup>3</sup>J. W. Shaner and E. B. Royce, *J. Appl. Phys.* **39**, 492 (1968).

<sup>4</sup>E. B. Royce, in *Physics of High Energy Density* (Academic, New York, 1971).

<sup>5</sup>G. E. Seay, R. A. Graham, R. C. Wayne, and L. D. Wright, *Bull. Am. Phys. Soc.* **12**, 1129 (1967).

<sup>6</sup>D. E. Grady, Preceding paper, *J. Appl. Phys.* **43**, 1942 (1972).

<sup>7</sup>L. C. Bartel, *J. Appl. Phys.* **40**, 3988 (1969).

<sup>8</sup>K. S. Aleksandrov and L. A. Aizenberg, *Sov. Phys. Dokl.* **11**, 323 (1966).

<sup>9</sup>W. Voigt, *Lehrbuch der Kristallphysik* (Terbner, Leipzig, 1928).

<sup>10</sup>A. Reuss, *Angew. Math. Mech.* **9**, 49 (1929).

<sup>11</sup>O. L. Anderson, in *Physical Acoustics*, edited by W. P. Mason (Academic, New York, 1965), Vol. III B.

<sup>12</sup>N. S. Akulov, *Z. Physik* **66**, 533 (1930).

<sup>13</sup>K. V. Vladimirov, *Dokl. Akad. Nauk SSSR* **41**, 10 (1943).

<sup>14</sup>E. W. Lee, *Rept. Progr. Phys.* **18**, 194 (1965).

<sup>15</sup>H. B. Callen and N. Goldberg, *J. Appl. Phys.* **36**, 976 (1965).

<sup>16</sup>This is strictly true only when the cubic material is isotropic ( $C_{11} - C_{12} = 2C_{44}$ ). For the magnetostriction effect there is extensive literature on this point (see Refs. 12-15). This literature does not apply to the inverse effect considered in the

- present article. A measure of the deviation from uniform strain can be calculated from the elastic constants of the bulk material and the isotropy factor of the cubic structure (see Ref. 36). It is small for YIG which has an isotropy factor of 0.95.
- <sup>17</sup>J. E. Knowles, *Brit. J. Appl. Phys.* **1**, 987 (1968).  
<sup>18</sup>R. Wadas, *Electron Tech. Warsaw* **2**, 63 (1969).  
<sup>19</sup>C. Kittel, *Rev. Mod. Phys.* **21**, 541 (1949).  
<sup>20</sup>Section II of Ref. 6.  
<sup>21</sup>R. R. Birss, *Proc. Phys. Soc. (London)* **75**, 8 (1960).  
<sup>22</sup>R. Carey and E. D. Isaac, *Magnetic Domains and Techniques for Their Observation* (Academic, New York, 1966).  
<sup>23</sup>E. W. Lee, *Proc. Phys. Soc. (London)* **72**, 249 (1959).  
<sup>24</sup>R. M. Bozorth, *Z. Physik* **124**, 519 (1947); *Phys. Rev.* **9**, 1788 (1953).  
<sup>25</sup>W. F. Brown, *Phys. Rev.* **53**, 482 (1938).  
<sup>26</sup>A more detailed description of this experimental method can be found in D. E. Grady, *Rev. Sci. Instr.* (to be published).  
<sup>27</sup>G. R. Fowles, G. E. Duvall, J. Asay, P. Bellamy, F. Feistmann, D. Grady, T. Michaels, and R. Mitchell, *Rev. Sci. Instr.* **41**, 984 (1970).  
<sup>28</sup>L. M. Barker and B. E. Hollenbach, *J. Appl. Phys.* **41**, 4208 (1970).  
<sup>29</sup>T. P. Liddiard, Jr., Fourth Symposium on Detonation, U.S. Naval Ordnance Laboratory, White Oak, Md., 1965 (unpublished).  
<sup>30</sup>D. E. Eastman, *Phys. Rev.* **148**, 530 (1966), and references therein.  
<sup>31</sup>G. E. Duvall and G. R. Fowles, in *High Pressure Physics and Chemistry*, edited by R. S. Bradley (Academic, New York, 1963), Vol. II.  
<sup>32</sup>Semi-Elements Inc., Saxonburg, Penn.  
<sup>33</sup>*Handbook of Microwave Ferrite Materials*, edited by W. H. vonAulack (Academic, New York, 1965), and references therein.  
<sup>34</sup>L. C. Bartel, *J. Appl. Phys.* **40**, 661 (1969).  
<sup>35</sup>R. C. Wayne, G. A. Samara, and R. A. Lefever, *J. Appl. Phys.* **41**, 633 (1970).  
<sup>36</sup>D. E. Grady, Ph.D. thesis (Washington State University, 1971) (unpublished).